MIXED TRANSFORM FINITE ELEMENT METHOD FOR SOLVING THE EQUATION FOR VARIABLY SATURATED FLOW

Robert G. Baca
Center for Nuclear Waste Regulatory Analyses
Southwest Research Institute, San Antonio, TX

Jacob N. Chung and David J. Mulla
Washington State University, Pullman, WA

ABSTRACT

A new computational method is developed for numerical solution of the nonlinear equation for variably saturated flow in porous media. The new method, referred to as the mixed transform finite element method, employs the mixed formulation of the Richards' equation but expressed in terms of a partitioned transform. An iterative finite element algorithm is derived using a Newton-Galerkin weak statement. Specific advantages of the new method are demonstrated with applications to a set of one-dimensional (1D) test problems. Comparisons with the modified Picard method show that the new method produces more robust solutions for a broad range of soil-moisture regimes, including unsaturated flow in desiccated soils, heterogeneous media, and variably saturated flow in layered soils with formation of perched water zones. In addition, the mixed transform finite element method is shown to converge faster than the modified Picard in a number of cases and to accurately capture pressure head and moisture content profiles with very steep fronts.

INTRODUCTION

The physics of isothermal, variably saturated flow in porous media is largely embedded in the mathematical symbolism referred to as Richards' equation (Jury et al., 1993). The descriptive capability of Richards' equation has popularized it as the "knowledge engine" for many 1D infiltration models (Celia, 1991; Stothoff, 1994), as well as for sophisticated three-dimensional unsaturated flow models (Runchal and Sagar, 1993; Ababou and Bagtzoglou, 1993). The generation of physical insights through high-resolution numerical simulations, however, has been limited because of the difficulty in obtaining

rapidly convergent and accurate numerical solutions for realistic problems. This is particularly the circumstance for simulation problems involving wetting fronts moving into a desiccated soil, unsaturated flow in layered soils with sharp contrasts in hydraulic properties, as well as the formation and dissipation of perched water zones.

Two primary sources of numerical difficulty are the strongly nonlinear nature of the Richards' equation and its unique mathematical character which can transition from parabolic, to hyperbolic, and elliptic behavior. The standard prescription for accommodating the nonlinearity has been to utilize an iterative method, such as a Newton-Raphson or Picard algorithm in conjunction with finite difference or finite element approximations (Huyakorn and Pinder, 1983). The ability of Richards' equation to simultaneously exhibit behavior of the three archetypal partial differential equations in the same simulation is particularly daunting. This mathematical character is a function of the flow regime and soil hydraulic properties. For earth materials with certain soil-moisture retention properties, capillarity will dominate moisture transport and, as result, the governing equation behaves like a nonlinear parabolic equation. In more drainable materials and relatively high saturation levels, gravity generally dominates and induces the propagation of a steep wetting front which is characteristic of a hyperbolic equation. In the case of fully saturated conditions, the governing equation simplifies to a linear elliptic equation. The "multiple personalities" of Richards' equation pose a special difficulty for the computational algorithm which must be capable of accommodating all three types of partial differential equations.

In this paper, the mixed transform finite element method is developed and applied to a set of challenging variably saturated flow problems. The capability of this new numerical method is demonstrated through direct comparisons with solutions produced with the widely popular modified Picard method (Celia et al., 1990).

GOVERNING FLOW EQUATION

The partial differential equation (PDE) for flow in a variably saturated porous medium was originally derived by Richards by combining the mass conservation equation with the Buckingham-Darcy flux law. Richards' equation provides an average macroscopic description of fluid flow processes that are essentially probabilistic in nature and occur at the microscopic level. In 1D form, the PDE is written as

$$\frac{\partial \theta}{\partial t} = \frac{\partial}{\partial z}\left[K(h)\left(\frac{\partial h}{\partial z} - 1\right)\right] \tag{1}$$

where θ is the volumetric water content (cm^3/cm^3), $K(h)$ the hydraulic conductivity (cm/s), z is the depth (cm) taken positive downward, and $h(\theta)$ the pressure head in centimeters of water. This PDE is commonly referred to as the mixed formulation of the variably saturated flow equation. Storage associated with compressibility of the porous medium and fluid is neglected in Eq. (1) although it can be easily and very effectively incorporated into Eq. (1), for example, using the approach of Paniconi et al. (1991).

Two alternate forms of this PDE are the so-called h- and θ-based PDEs (Jury et al., 1993). The standard h-based formulation, which is the more popular of the two, is expressed as:

$$C(h)\,\frac{\partial h}{\partial t} = \frac{\partial}{\partial z}\left[K(h)\left(\frac{\partial h}{\partial z} - 1\right)\right] \tag{2}$$

with the moisture capacity term defined as $C(h) = \partial\theta/\partial h$. The θ-based formulation is:

$$\frac{\partial \theta}{\partial t} = \frac{\partial}{\partial z}\left[D(\theta)\frac{\partial \theta}{\partial z} - K\right] \tag{3}$$

with the moisture diffusivity defined as $D(\theta) = K(\theta)/C(\theta)$. The classical h-based formulation has the advantage of being applicable to both saturated and unsaturated conditions, and accommodating heterogeneous soils. However, numerical approximations of this formulation generally exhibit very poor preservation of global mass balance (Celia et al., 1990; Milly, 1985) and relatively slow convergence. In

contrast, the classical θ-based formulation is limited to homogeneous media and strictly unsaturated conditions. When discretized, however, it produces very well behaved and rapidly convergent solutions (Selim, 1971).

Celia et al. (1990) developed a semi-discrete "delta" formulation of Eq. (1), which is referred to as the modified Picard method. This method apparently combines the benefits of both h- and θ-based PDEs without the inherent drawbacks of each formulation. Of particular importance is the mass conservative nature of this delta formulation. This formulation is expressed mathematically as:

$$C(h)\frac{\delta}{\Delta t} = \frac{\partial}{\partial z}\left[K(h)\left(\frac{\partial \delta}{\partial z} - 1\right)\right] + \frac{\partial}{\partial z}\left[K(h^k)\frac{\partial h^k}{\partial z}\right] - \frac{\Delta\theta^k}{\Delta t} \tag{4}$$

where $\delta = h^{k+1} - h^k$ and k is the iteration index.

Similarly, Hills et al. (1989) and Kirkland et al. (1992) harvested the advantages of both the h- and θ-based formulations by introducing a generalized variable Φ which is a linear transform of pressure head and moisture content. They derive a modified form of the Richards' equation, namely

$$F\frac{\partial \Phi}{\partial t} = \frac{\partial}{\partial z}\left(\frac{K}{G}\frac{\partial \Phi}{\partial z} - K\right) - \frac{\partial}{\partial z}\left(\frac{K}{G}\frac{\partial g}{\partial z}\right) \tag{5}$$

where $\Phi = \Phi(z,t) = g[h(z,t),z]$, $\theta = \theta(z,t) = f[h(z,t),z]$, $F = \partial f/\partial h \; \partial h/\partial \Phi$, and $G = \partial g/\partial h$. The last term in Eq. (5) accounts for the "jump conditions" in the soil properties at layer interfaces. Because Eq. (5) requires that Φ be uniquely defined, it can only be solved using a finite volume analog with cell-centered nodes so that discontinuous changes occur at the cell interface. Other disadvantages of this approach are associated with the calculation of G and $\Delta\Phi$ at the layer interfaces (Kirkland et al., 1992).

In this paper, it is demonstrated that the modified PDE expressed in Eq. (5) is unnecessary and a finite element analog can indeed be used with node points located at the material interfaces. In addition,

the computational advantages of the new mixed transform method are illustrated through comparisons against the modified Picard method.

MIXED TRANSFORM FORMULATION

Using ideas similar to that of Kirkland et al. (1992), a mixed formulation of Richards' equation can be developed in terms of the transformed variable χ:

$$\frac{\partial \theta}{\partial t} = \frac{\partial}{\partial z}\left(K\frac{\partial h}{\partial \chi}\frac{\partial \chi}{\partial z} - K\right) \tag{6}$$

where

$$\chi = \begin{cases} -h & h \geq h_0 \\ \alpha_1\theta + \alpha_2 & h < h_0 \end{cases} \tag{7}$$

with the transform constants

$$\frac{\partial h}{\partial \chi} = \begin{cases} -1 & h \geq h_0 \\ 1/\alpha_1 C(h) & h < h_0 \end{cases} \tag{8}$$

$$\alpha_1 = \frac{-1}{C(h_0)} \tag{9}$$

$$\alpha_2 = -h_0 - \alpha_1\theta_0 \tag{10}$$

The transition pressure head h_0 is an arbitrary parameter with θ_0 being the corresponding water content value. It is easy to verify that for $h \geq h_0$, direct substitution of Eqs. (7) and (8) into Eq. (6) yields the h-based form. Similarly, for $h < h_0$, Eq. (6) transforms to the θ-based form. To fully exploit the benefits of the partitioned transform, the transition pressure is chosen to be close to the air entry pressure. This

particular choice of h_0 has the effect of making the transformed PDE behave (numerically) much more like the classical θ-based formulation expressed in Eq. (3).

FINITE ELEMENT ALGORITHM

An iterative finite element algorithm is formulated using the elegantly simple Galerkin procedure which requires that the integral over the domain of the residual, ϵ, and a set of weighting functions, ω_j, vanishes. Thus, the Galerkin functional is

$$\Omega_G = \int_0^L \omega_j \epsilon \, dz = 0 \tag{11}$$

where the residual is obtained directly from Eq. (6), namely

$$\epsilon = \frac{\partial \theta}{\partial t} - \frac{\partial}{\partial z}\left(K \frac{\partial h}{\partial \chi} \frac{\partial \chi}{\partial z} - K \right) \tag{12}$$

In this expression, the quantities θ, χ, and K are approximated in terms of a set of linear basis functions; these functions are chosen to be identical to the set of weighting functions ω_j. Since the residual is nonlinear, it is useful to expand ϵ in terms of a Taylor series (Baca et al., 1978). Thus, the Newton-Galerkin functional is

$$\Omega_{NG} = \int_0^L \omega_j \left(\epsilon^{(k)} + \frac{\partial \epsilon^{(k)}}{\partial h} \Delta h \right) dz = 0 \tag{13}$$

where k is the iteration index. It is important to note that the Taylor series is expanded in terms of h rather than θ or χ, which are discontinuous. Choosing h as the solution variable has the advantage cited previously for the h-based formulation. The nodal values of pressure head h_j at the new iterate $k+1$ and the new time plane $n+1$ are computed using the Newton iteration formula:

$$h_j^{(k+1)} = h_j^{(k)} + \Delta h_j \tag{14}$$

In certain problems, convergence can be improved by use of a "damped" Newton iteration in which Δh_j is limited to a maximum value. There are a number of approaches (Jenning and McKeown, 1992) for computing the appropriate level of damping. A simple and direct approach consists of computing the incremental change according to

$$\Delta h_j^{\min} = \min(|\Delta h_j|, f|h_j|) \tag{15}$$

where the damping factor $f \leq 1$. The appropriate sign is recovered from $\Delta h_j = sign\left(\Delta h_j^{\min}, \Delta h_j\right)$.

Rearranging the quantities in Eq. (13) and expressing them in matrix notation produces:

$$[J]\{\Delta h\} = -\{R\} \tag{16}$$

where the right-hand side vector, $\{R\}$, and Jacobian matrix, $[J]$, are:

$$\{R\} = \int_0^L \omega_j \epsilon^{(k)} dz \qquad \{J\} = \int_0^L \omega_j \frac{\partial \epsilon^{(k)}}{\partial h} dz \tag{17}$$

Discretizing $\partial\theta/\partial t$ and integrating by parts, the components of the Newton-Galerkin "weak statement" become

$$\{R\} = \frac{1}{\Delta t}\int_0^L \omega_j \left(\theta^{n+1} - \theta^n\right) dz + \int_0^L \frac{\partial \omega_j}{\partial z}\left(K\frac{\partial h}{\partial \chi}\frac{\partial \chi}{\partial z} - K\right) dz - \omega_j\left(K\frac{\partial h}{\partial \chi}\frac{\partial \chi}{\partial z} - K\right)_0^L \tag{18}$$

$$[J] = \frac{1}{\Delta t}\int_0^L \omega_j \frac{\partial \theta^{n+1}}{\partial h} dz + \int_0^L \frac{\partial \omega_j}{\partial z}\left(K\frac{\partial h}{\partial \chi}\frac{\partial}{\partial h}\left(\frac{\partial \chi}{\partial z}\right) - \frac{\partial K}{\partial h}\right) dz \tag{19}$$

The integration by parts, in the previous equations, effectively reduced or "weakened" the differentiation requirement (Pepper and Heinrich, 1992) on χ. Inserting the standard expressions for the linear basis functions, Eqs. (18) and (19) can be integrated exactly. For a generic finite element of length L_e, the elemental matrices are:

$$\{R_e\} = \frac{1}{\Delta t}\left(\frac{L_e}{2}\right)\begin{bmatrix}1 & 0\\ 0 & 1\end{bmatrix}\left(\{\theta\}^{n+1} - \{\theta\}^{n}\right) + \frac{1}{L_e}\left(\frac{\kappa_1+\kappa_2}{2}\right)\begin{bmatrix}1 & -1\\ -1 & 1\end{bmatrix}\{\chi\} - \left(\frac{K_1+K_2}{2}\right)\begin{Bmatrix}-1\\ 1\end{Bmatrix} - \begin{Bmatrix}q_0^{bc}\\ -q_L^{bc}\end{Bmatrix} \tag{20}$$

$$[J_e] = \frac{1}{\Delta t}\left(\frac{L_e}{2}\right)\begin{bmatrix}\partial\theta_1/\partial h & 0\\ 0 & \partial\theta_2/\partial h\end{bmatrix} + \frac{1}{L_e}\left(\frac{\kappa_1+\kappa_2}{2}\right)\begin{bmatrix}\partial\chi_1/\partial h & -\partial\chi_2/\partial h\\ -\partial\chi_1/\partial h & \partial\chi_2/\partial h\end{bmatrix} - \frac{1}{2}\begin{bmatrix}-\partial K_1/\partial h & -\partial K_2/\partial h\\ \partial K_1/\partial h & \partial K_2/\partial h\end{bmatrix} \tag{21}$$

where $\kappa = K\partial h/\partial\chi$. In deriving the above expression, the derivatives of κ have been neglected because they result in products of first order terms that are small. The boundary flux terms q_0^{bc} and q_L^{bc} are zero everywhere except at the top and the bottom boundaries, if specified. Mass lumping has been used in Eqs. (20) and (21) to stabilize the matrices associated with the θ-terms.

In implementing the new finite element algorithm, termination of the Newton iteration process is based on a dual convergence criteria which tests the norms of relative change and residual vectors. Specifically, the numerical solution must satisfy:

$$\max\ |\Delta h_j/h_j| \le \epsilon_{\text{rel}} \quad \text{and} \quad \|r^{(k+1)}\|_\infty \le \epsilon_{\text{res}} \tag{22}$$

where $\|\ \|_\infty$ is the infinity norm and $r^{(k+1)}$ is the residual computed as $J\Delta h^{(k+1)} + R$.

In general, the maximum relative change is a good indicator of convergence: however, the residual norm is more stringent and reliable. Typical values of the control tolerances are $10^{-5} \leq \epsilon_{rel} \leq 10^{-3}$ and $10^{-8} \leq \epsilon_{res} \leq 10^{-5}$.

COMPUTATIONAL TEST PROBLEMS

Three challenging computational test problems, taken directly from the hydrology literature, were solved to demonstrate the capabilities of the mixed transform finite element code. For the purpose of making comparisons, numerical solutions were also generated using two distinct 1D codes that utilize the modified Picard method. The two codes were the UNSAT1D code (Celia, 1991) and BREATH code (Stothoff, 1994). Both of these codes utilize the modified Picard algorithm described in Celia et al. (1990). Two primary differences between these independent codes and the mixed transform finite element code are associated with the convergence criteria and the spatial approximation of hydraulic properties. Those differences are subsequently described.

The computational difficulties associated with the selected test problems can be characterized in terms of the grid hydraulic Peclet number Pe_{hg} and hydraulic time scale parameter τ_{hg}. As in heat and mass transfer, the hydraulic Peclet number (Finlayson, 1980; Ababou, 1990) describes the relative significance of convective to diffusive transport. A large Peclet number $Pe_{hg} > 2$ means that the gravity term in Richards' equation is dominant and implies that a fine grid may be necessary to capture a sharp pressure front. The grid hydraulic Peclet number is calculated from:

$$Pe_{hg} = -\frac{\partial}{\partial h}[\ln K(h)]\Delta z \tag{23}$$

where Δz is the element size. In diffusion or capillarity dominated moisture transport, the hydraulic time scale parameter is an approximate indicator of the characteristic hydraulic response time for a computational element. This quantity is computed from

$$\tau_{hg} = \frac{\Delta z^2}{K(h)/C(h)} \tag{24}$$

Zones at or near saturated conditions generally exhibit smaller characteristic times and, thus, control the time stepping for the entire domain. Typically, the maximum time step should be chosen to be some fraction of $3\tau_{hg}$ to capture the transient changes in pressure head occurring across an element.

Test Problem 1 – Unsaturated Flow into a Desiccated Soil Column

The first computational problem is adapted from an unsaturated flow simulation previously used by Celia et al. (1990) to test numerical techniques for solving Richards' equation. This test problem involves modeling a wetting front moving through a homogeneous, vertical soil column. This deceptively simple flow problem is fairly challenging because of the imposed Dirichlet boundary conditions, strongly nonlinear soil hydraulic properties, and relatively large pressure head gradients. The idealized soil column is 60 cm in length and is assumed to consist of desert soil representative of the Las Cruces field site in New Mexico. Flow in the soil column occurs as a result of the specified pressure head at the surface, gravity, and capillarity effects. The bottom boundary is held at the initial pressure head, h_i. Soil hydraulic properties are described by the van Genuchten (1980) relations:

$$S_e = \frac{\theta - \theta_r}{\theta_s - \theta_r} = \left[\frac{1}{1 + (\alpha |h|)^n} \right]^m \tag{25}$$

$$K = K_s S_e^{1/2} \left[1 - \left(1 - S_e^{1/m} \right)^m \right]^2 \tag{26}$$

where θ_r and θ_s are residual and saturated water contents, respectively, K_s is the saturated hydraulic conductivity, and α, n, and m are model parameters with $m = 1 - 1/n$. Values for these parameters are $\theta_r = 0.102$, $\theta_s = 0.368$, $K_s = 0.00922$ cm/s, $\alpha = 0.0335$ 1/cm, and $n = 2$.

To make the problem progressively more challenging, three cases were computed in which the top boundary pressure, h_b, was varied, namely $h_b = -75$, -25, and 0 cm. The initial pressure head in the soil column was uniform and set to a value of $h_i = -1{,}000$ cm. A uniform mesh of 2-node line elements was used to represent the vertical soil column with $\Delta z = 2.5$ cm. The mixed transform simulation was performed using variable time stepping ranging from $\Delta t = 10$ to 100 s. Convergence of the iteration algorithm was defined by the tolerances $\epsilon_{rel} \leq 10^{-4}$ and $\epsilon_{res} \leq 10^{-5}$. The UNSAT1D code (Celia, 1991) determines convergence based on the maximum relative change, $\max |\Delta h_j / h_j|$ and the infinity norm of the right-hand side, $\|\boldsymbol{R}\|_\infty$. Consequently, the convergence criteria were only approximately equivalent to those used in the mixed transform finite element code, namely Eq. (22).

Numerical results for the three cases are summarized in Figure 1, which compares the pressure head profiles obtained with the mixed transform method and the modified Picard method. Overall, this graphical comparison shows satisfactory agreement except in the location of the front. To resolve this difference, the UNSAT1D simulation was repeated with a finer grid and smaller time steps. The fine grid solution, also presented in Figure 1, shows closer agreement with the mixed transform solution. Iteration histories for the two bounding cases are compared in Figure 2. These histories suggest that the mixed transform method exhibits much faster convergence for the case of the "wet" boundary condition ($h_b = 0$ cm) while the modified Picard method is more competitive (i.e., faster convergence and less sensitivity to time step size) for the "dry" boundary condition ($h_b = -75$ cm) case. In terms of cpu time, the mixed transform solution for the wet case was about twice as fast as the modified Picard solution, whereas, it required about 30 percent more cpu time for the dry case.

Insight into the numerical characteristics of this test problem is provided in Figure 3 which shows the $\boldsymbol{Pe}_{hg}$ and τ_{hg} curves for the three cases. Progressing from the dry boundary condition to the

wet boundary condition, the Pe_{hg} curves show an increasingly rapid change to the maximum value (~ 900 not shown in figure) and formation of regions behind the front of zero and near zero values. Similar trends are exhibited by the τ_{hg} curves. In the wet boundary condition case, a large portion of the soil column exhibits $\tau_{hg} = 0$ which means that the flow equation has degenerated to steady state (i.e., elliptic) in this region. The flow equation is fully transient (and parabolic to hyperbolic) at and ahead of the front, explaining the observed progressive sensitivity to time step illustrated in Figure 2.

Test Problem 2 – Unsaturated Flow into a Dry Layered Soil

The second test problem, originally solved by Hills et al. (1989), involves modeling infiltration into a field scale layered lysimeter. This test problem is an excellent one because it poses a strongly nonlinear unsaturated flow problem that exhibits very large gradients in both pressure head and moisture content. The flow regime is driven by a constant flux boundary condition of $q_0^{bc} = 2$ cm/d at the soil surface. Five soil layers (each 20 cm) consisting of alternating Bernino loamy fine sand and Glendale clay loam make up the 100-cm soil column. Soil hydraulic properties are described by the van Genuchten (1980) formulas. For the Bernino loamy fine sand, these parameters are $\theta_r = 0.0286$, $\theta_s = 0.3658$, $K_s = 541.0$ cm/d, $\alpha = 0.0280$ 1/cm, and $n = 2.2390$. For the Glendale clay loam, the soil hydraulic parameters are $\theta_r = 0.1060$, $\theta_s = 0.4686$, $K_s = 13.1$ cm/d, $\alpha = 0.0104$ 1/cm, and $n = 1.3954$.

Two cases of increasing computational difficulty were simulated in which the initial pressure head profile was set to $h_i = -10{,}000$ and $-50{,}000$ cm. The bottom boundary was held at the initial pressure head. The flow domain was discretized into a uniform mesh of finite elements with $\Delta z = 1$ cm. A time domain of 5 days was simulated using variable time stepping ranging from $\Delta t = 10$ to 100 s. The

convergence tolerances were set to $\epsilon_{rel} \leq 10^{-5}$ and $\epsilon_{res} \leq 10^{-6}$. In running this test problem with the UNSAT1D code, the arithmetic averaging option was used for calculation of interlayer conductivities.

The moisture content profiles computed for the two are shown in Figure 4 for t = 5.0 days. In this figure, the numerical results obtained for both cases with the mixed transform code are compared with those obtained with the UNSAT1D code. The results produced by the mixed transform finite element method match nearly perfectly with those computed with the modified Picard method. At depths of 60 to 65 cm, the two moisture profiles differ very slightly because of differences in the shapes of the pressure fronts, which are compared in Figure 5. Although both cases exhibit very large pressure gradients, quite interestingly, neither case was especially taxing for either the mixed transform or modified Picard method. The comparison of cpu times for the first case showed that the modified Picard solution was about 3.5 times faster than the mixed transform solution, while for the second case, it was about 5.5 times faster. This comparison of cpu times clearly shows the superiority of the modified Picard method for problems with low infiltration rates and very dry initial conditions.

The Pe_{hg} and τ_{hg} curves for the two cases were found to be quite similar with the main differences being the maximum values. It was noted that the Peclet number and time scale parameter values for this test problem are more constraining at the end of the simulation than at the beginning. The curves for t = 5 days and h_i = −10,000 are illustrated in Figure 6; they suggest that the first two layers are largely capillary dominated and exhibit the smaller hydraulic response times.

Test Problem 3 – Variably Saturated Flow into a Layered Soil

The final test problem is taken from Ross and Bristow (1990) and involves flow into a layered soil column. A high flux boundary condition, relative to the soil hydraulic conductivity, creates locally saturated and unsaturated flow regimes. The physical setting consists of a surface crust (0.5 cm), a tilled layer (10 cm), and an undisturbed subsoil layer (15 cm). At the surface, the water application rate is

q_0^{bc} = 10 cm/h while the bottom boundary is held at a fixed pressure head value equal to the initial value.

The soil hydraulic properties for each layer are described by the formulas (Campbell, 1985):

$$\theta(h) = \begin{pmatrix} \theta_s & h \geq h_a \\ \theta_s (h/h_a)^{-1/b} & h < h_a \end{pmatrix} \tag{27}$$

$$K(h) = \begin{pmatrix} K_s & h \geq h_a \\ K_s (h/h_a)^{-n} & h < h_a \end{pmatrix} \tag{28}$$

where h_a is the air entry value of pressure head, and b and n are fitting parameters with $n = 2 + 3/b$. The parameter values for: (i) the surface crust are θ_s = 0.562, K_s = 0.0616 cm/hr, h_a = −4.55 cm, and b = 6.8; (ii) the tilled layer are θ_s = 0.562, K_s = 1.396 cm/hr, h_a = −4.55 cm, and b = 13.3; and (iii) the undisturbed subsoil are θ_s = 0.440, K_s = 0.312 cm/hr, h_a = −9.50 cm, and b = 13.3.

The vertical soil column was represented by a variably spaced finite element mesh consisting of Δz = 0.25 cm in the surface crust, Δz = 0.5 cm in the tilled layer, and Δz = 0.5 to 1.0 cm in the undisturbed subsoil layer. The initial pressure head was uniform and set to h_i = −35,100 cm. In setting up the BREATH code (Stothoff, 1994) for this problem, a slightly finer grid was necessary because the code uses "node based" hydraulic properties; small elements were used to straddle the layer interfaces. A total time period of 7 hr was simulated using variable time steps of Δt = 10 to 200 s. Convergence of the mixed transform iteration algorithm was defined by the tolerances $\epsilon_{rel} \leq 10^{-5}$ and $\epsilon_{res} \leq 10^{-6}$. In the BREATH code, convergence is determined on the basis of maximum relative change only. Thus, the convergence criteria between the two computational methods was only partially equivalent.

The computed moisture content profiles for t = 7.0 hr are illustrated in Figure 7. In this figure, the numerical solutions produced by the mixed transform finite element method are compared with those

calculated with the BREATH finite element code. The differences between the two moisture profiles are very small. The calculated pressure head profiles, which are presented in Figure 8, also show excellent agreement. The iteration histories. which are presented in Figure 9, give insight to the computational efficiency of the two solution techniques. From this plot, it can be noted that the modified Picard method exhibits a much greater sensitivity to time step size for this case. In fact, for the large time step size the Picard iteration process shows a large increase in iterations. This behavior is consistent with the iteration history observed in the first test problem. The comparison of cpu times showed that the mixed transform solution was about 1.6 times faster than the modified Picard solution.

The Pe_{hg} and τ_{hg} curves calculated for this test problem were found to be relatively simple and showed that this problem was primarily dominated by capillary flow and the hydraulic response times were very large for the entire simulation period. These numerical characteristics explain, to some degree, the observation of Ross and Bristow (1990) that accurate solutions for this test problem can be obtained with a coarse grid and large time steps.

SUMMARY AND CONCLUSIONS

A mixed transform finite element method was developed for solving Richards' equation for variably saturated flow. In this new approach, the mixed formulation of the flow equation is transformed using a partitioned change of variable. An iterative scheme is embedded in the finite element algorithm for the transformed equation. This technique is formulated using a Newton-Galerkin weak statement. The capabilities of this new method are demonstrated with applications to a set of challenging 1D computational test problems. For the broad range of regimes considered in the test cases, the mixed transform method exhibits a higher degree of robustness than the modified Picard method. In certain cases, the mixed transform method can converge faster and more accurately capture steep pressure head and moisture content profiles, which are typically encountered in desiccated soils. The new method is easy to implement in existing one- and multi-dimensional finite element codes, as well as finite volume codes.

Although the new method offers improved computational efficiency, accuracy, and reliability for a broad class of variably saturated flow problems, it must be acknowledged that the modified Picard method may be more competitive (i.e., allows larger time steps) for certain cases of strictly unsaturated flow conditions. This suggests that an even more robust computational technique might be constructed by combining both methods, possibly through a linear weighting of the element stiffness matrices. Such an approach is being explored and may be the topic of a future publication.

ACKNOWLEDGMENTS

The author wishes to thank Drs. S. Stothoff, P. Lichtner, and G. Ofoegbu for their review and comments on the original manuscript. The assistance of Dr. Stothoff with the application of the BREATH code is gratefully acknowledged. The research presented in this paper was funded by the Nuclear Regulatory Commission (NRC) under Contract No. 02-93-005 and was performed at the Center for Nuclear Waste Regulatory Analyses (CNWRA). The research was performed on behalf of the NRC Office of Nuclear Regulatory Research, Division of Regulatory Applications. The paper is an independent product of the CNWRA and does not necessarily reflect the views or regulatory position of the NRC. The BREATH code used in this study is controlled under the CNWRA Software Configuration Procedure. The other codes used in the study are not yet under software configuration management.

REFERENCES

Ababou, R., Numerical analysis of nonlinear unsaturated flow equation, *Proceedings of Computational Methods in Subsurface Hydrology,* Springer-Verlag, Berlin, 151–159, 1990.

Ababou, R., and A.C. Bagtzoglou, *BIGFLOW: A Numerical Code for Simulating Flow in Variably Saturated, Heterogeneous Geologic Media, Theory and User's Manual, Version 1.1,* NUREG/CR-6028, Nuclear Regulatory Commission, Washington, DC, 1993.

Baca, R.G., I.P. King, and W.R. Norton. Finite element models for simultaneous heat and moisture transport in unsaturated soils. *Proceedings of the Second International Conference on Finite Elements in Water Resources*. Pentech Press, London, UK, 1.19–1.35, 1978.

Campbell, G.S., *Soil Physics with BASIC*. Elsevier, New York, NY, 1985.

Celia, M.A., E.T. Bouloutas, and R.L. Zarba, A general mass-conservative numerical solution for the unsaturated flow equation. *Water Resour. Res.*, 26(7), 1483–1496, 1990.

Celia, M.A., *The One-Dimensional Princeton Unsaturated Flow Code*, Distributed at the Short Course on Fundamentals of Unsaturated Zone Modeling, Princeton University, Princeton, NJ, 1991.

Finlayson, B.A., *Nonlinear Analysis in Chemical Engineering*, McGraw-Hill International Book Company, New York, NY, 1980.

Hills, R.G., I. Porro, D.B. Hudson, and P.J. Wierenga, Modeling one-dimensional infiltration into very dry soils, 1. Model development and evaluation, *Water Resour. Res.*, 25(6), 1259–1269, 1989.

Haverkamp, R., M. Vauclin, J. Touma, P.J. Wierenga, and G. Vachaud, A comparison of numerical simulation models for one-dimensional infiltration, *Soil Sci. Soc. Am. J.* 41, 285–294, 1977.

Huyakorn, P.S., and G. Pinder, *Computational Methods in Subsurface Flow*, Academic Press, Inc., New York, NY, 1983.

Jenning, A., and J.J. McKeown, *Matrix Computation*, John Wiley & Sons, New York, NY, 1992.

Jury, W.A., W.R. Gardner, and W.H. Gardner, *Soil Physics*, Fifth Edition, John Wiley & Sons., New York, NY, 1993.

Kirkland, M.R., R.G. Hills, and P.J. Wierenga, Algorithms for solving Richards' equation for variably saturated soils, *Water Resour. Res.*, 28(8), 2049–2058, 1992.

Milly, P.C.D., A mass-conservative procedure for time-stepping in models of unsaturated flow, *Adv. Water Resour.*, 8, 32–36, 1985.

Paniconi, C., A.A. Aldama, and E.F. Wood, Numerical evaluation of iterative and noniterative methods for the solution of the nonlinear Richards equation, *Water Resour Res.*, 27(6), 1147–1163, 1991.

Pepper, D.W., and J.C. Heinrich, The Finite Element Method, Taylor and Francis Publishing, Bristol, PA, 1992.

Ross, P.J., and K.L. Bristow, Simulating water movement in layered and gradational soils using the Kirchhoff transform, *Soil Sci. Soc. of Am. J.*, 54, 1519–1524, 1993.

Runchal, A.K., and B. Sagar, *PORFLOW—A Multifluid, Multiphase Model for Simultaneous Flow, Heat Transfer, and Mass Transport in Fractured-Porous Media, User's Manual, Version 2.41*, NUREG/CR-5991, Nuclear Regulatory Commission, Washington, DC, 1993.

Selim, H.M.E., *Transient and Steady Two-Dimensional Flow of Water in Unsaturated Soils*, Ph.D. Thesis, Iowa State University, Ames, IA, 1971.

Stothoff, S., *Breath Version 1.0—Coupled Flow and Energy Transport in Porous Media, Simulator Description and User Guide*, CNWRA 94-020, Center for Nuclear Waste Regulatory Analyses, Southwest Research Institute, San Antonio, TX, 1994.

van Genuchten, M.T., A closed-form equation for predicting the hydraulic properties of unsaturated soils, *Soil Sci. Soc. Am. J.*, 44, 892–898, 1980.

Fig. 1. Comparison of mixed transform and modified Picard solutions for 3 cases specified for test problem 1: $h_b = -75, -25, 0$ cm.

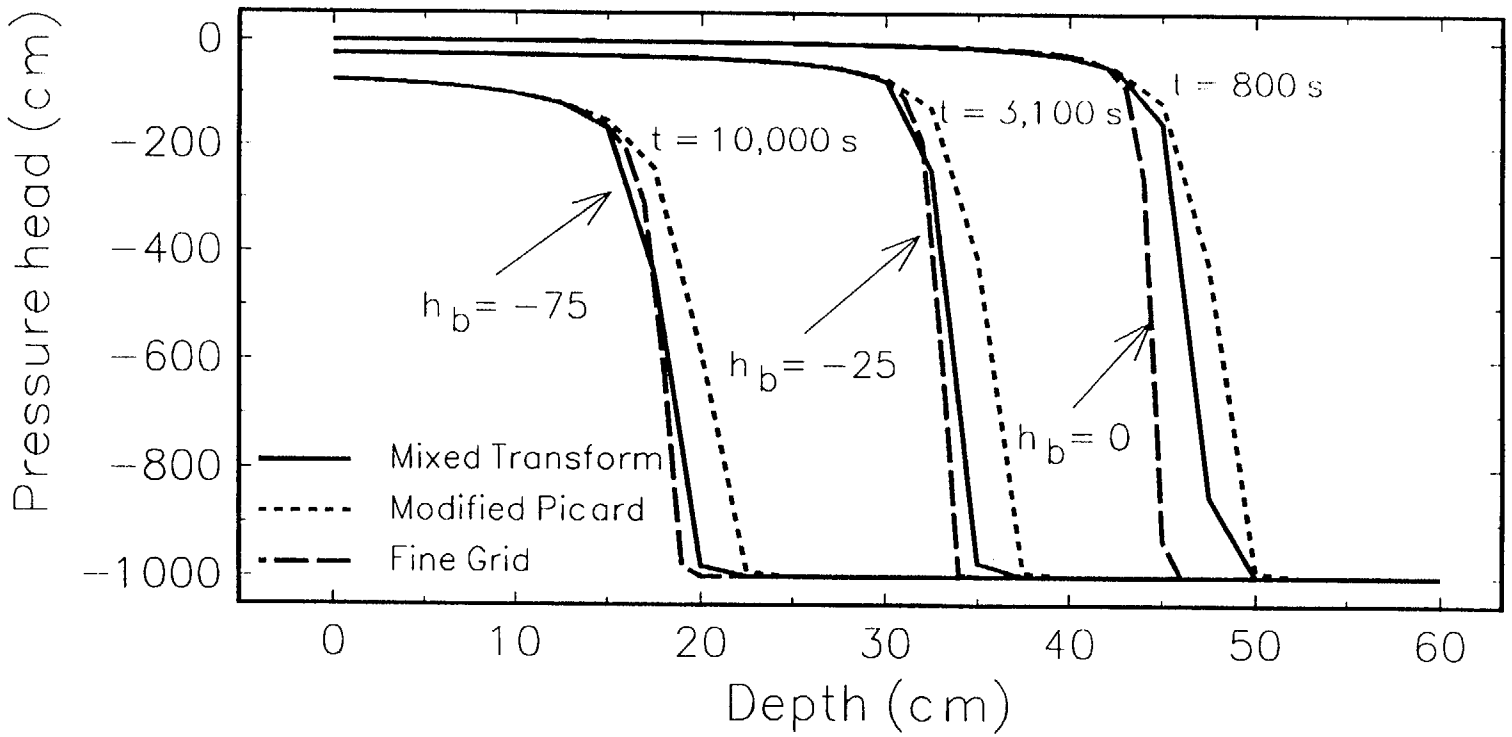

Fig. 2. Iteration histories for mixed transform and modified Picard solutions for bounding cases of test problem 2.

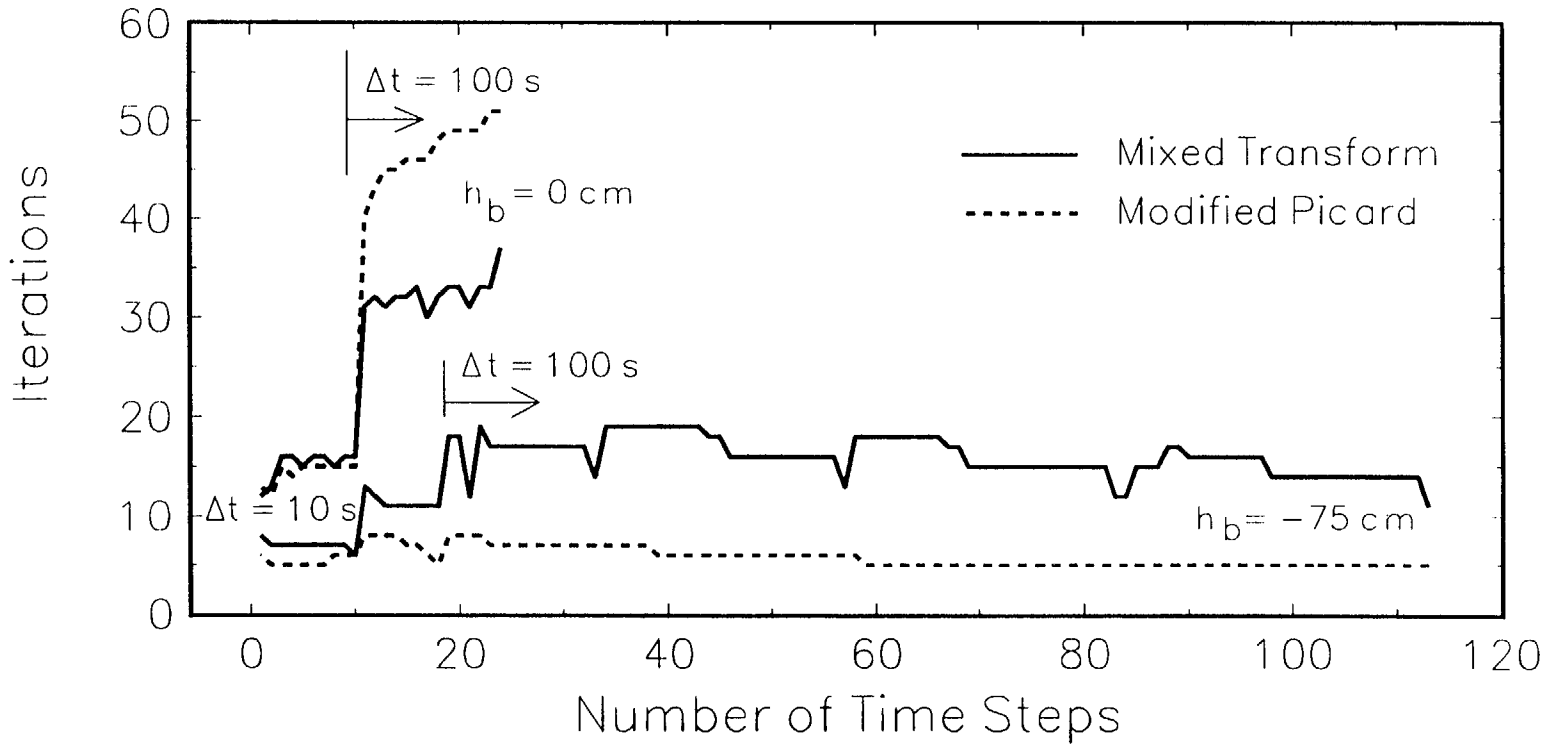

Fig. 3. Hydraulic Peclet number and time scale curves for 3 cases of test problem 1.

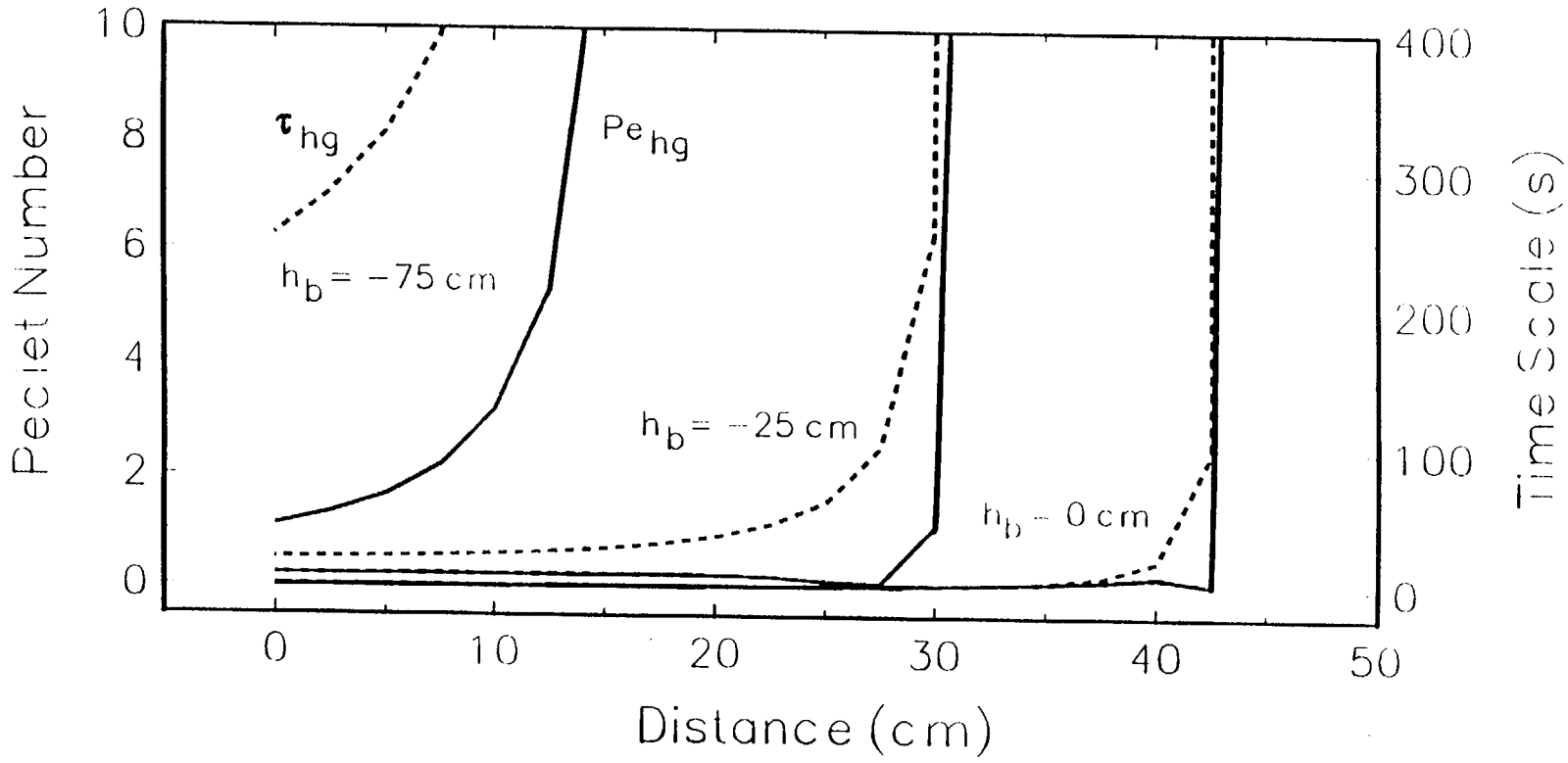

Fig. 4. Moisture content profiles computed for test problem 2 using the mixed transform and modified Picard methods.

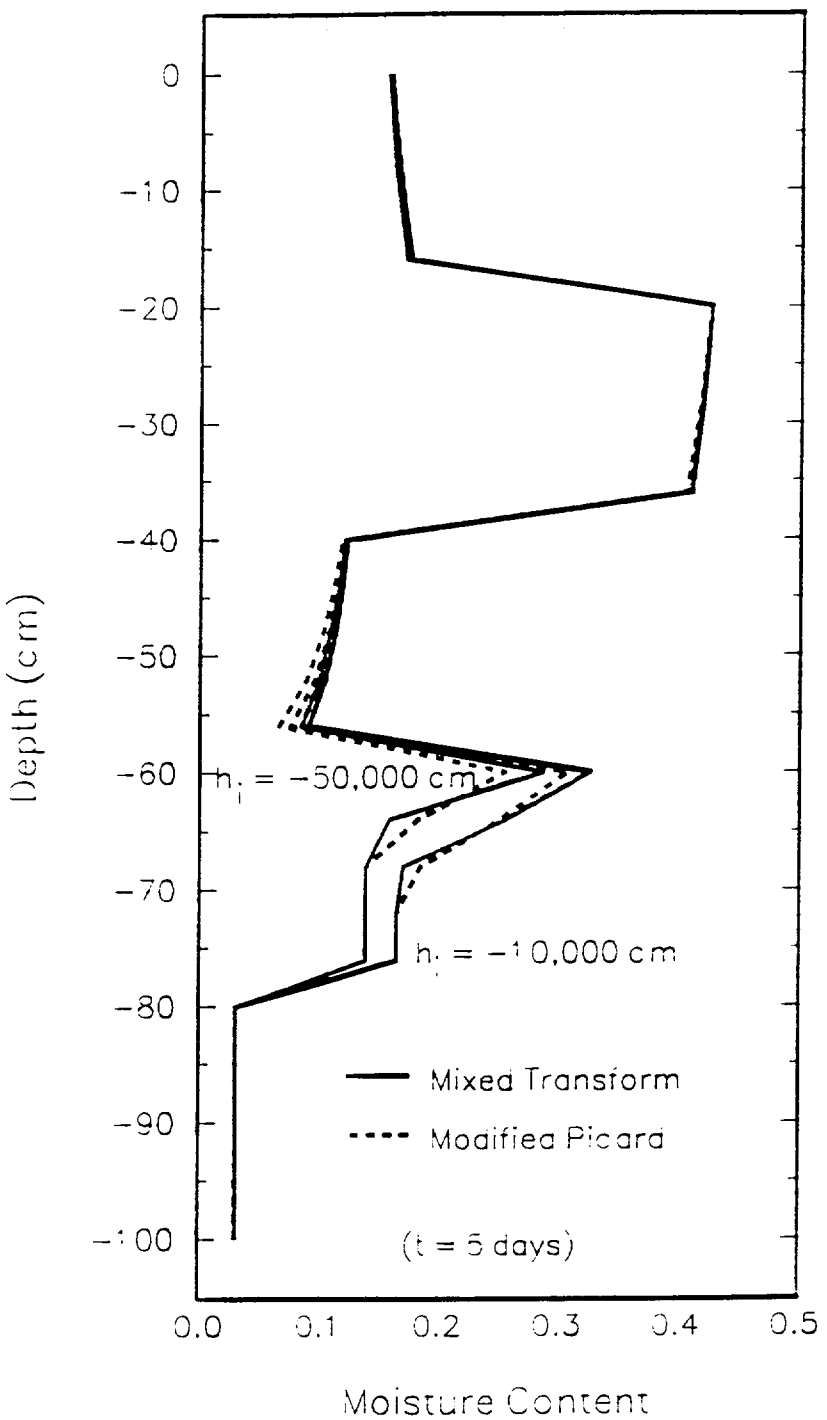

Fig. 5. Comparison of pressure head profiles computed for two cases of test problem 2.

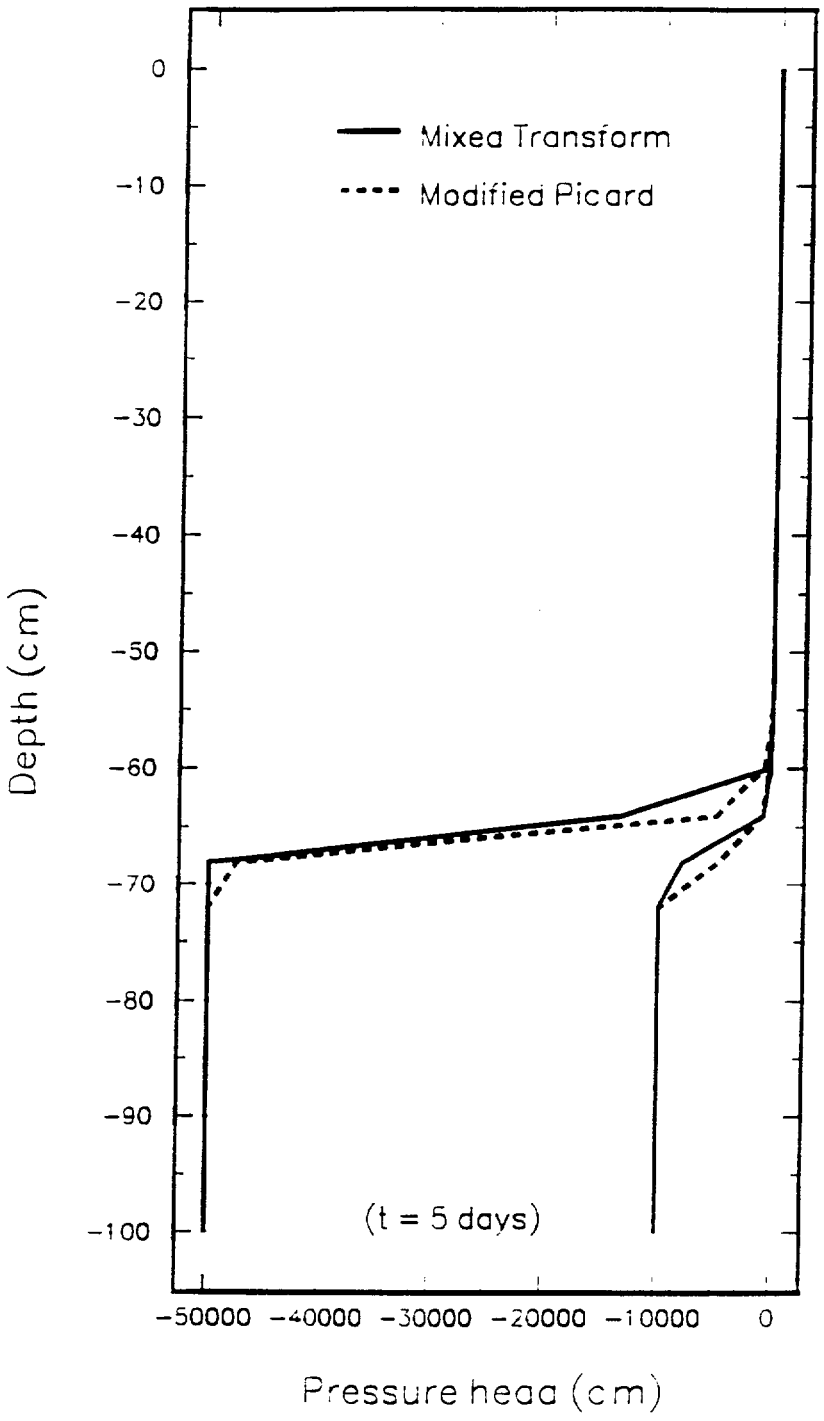

Fig. 6. Hydraulic Peclet number and time scale curves for test problem 2.

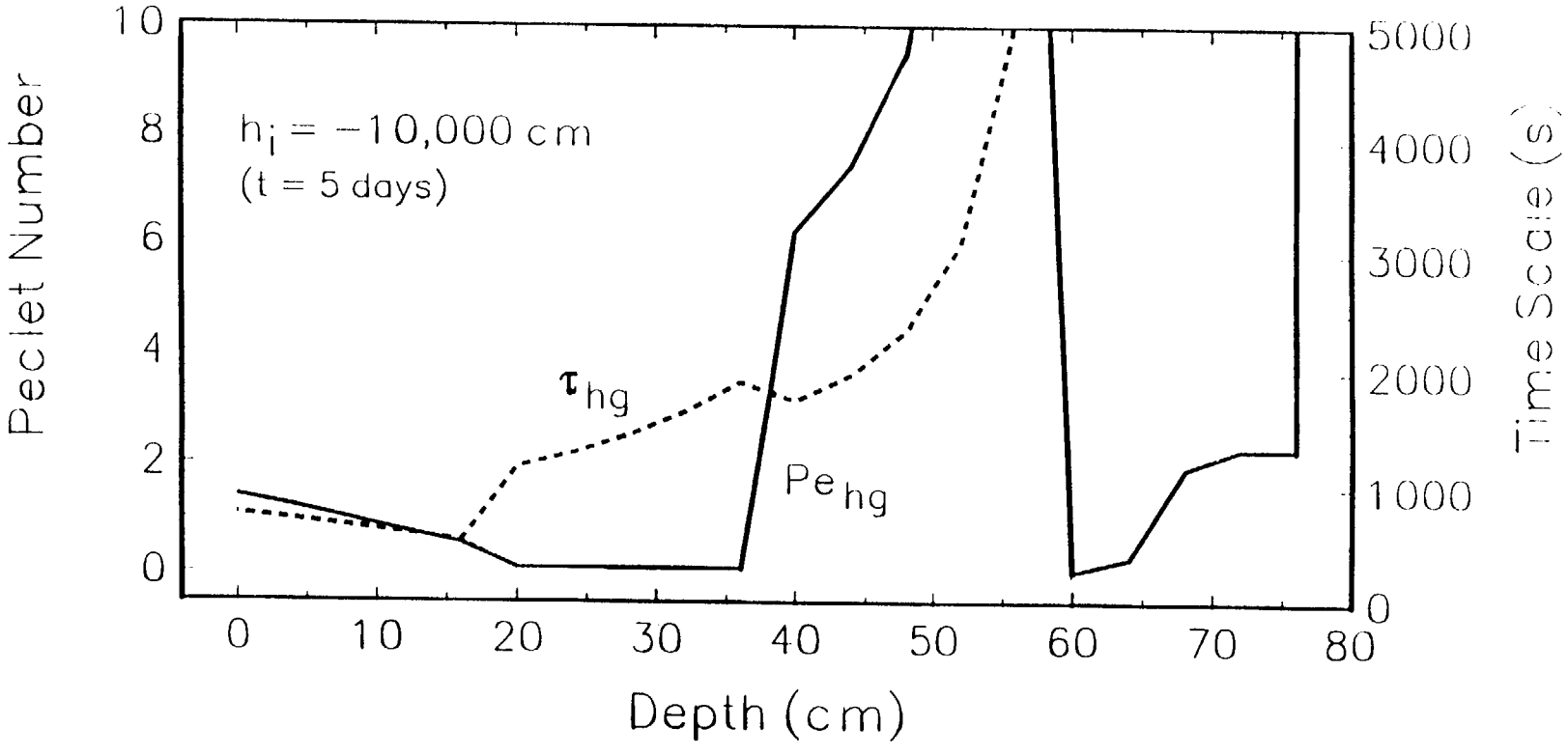

Fig. 7. Comparison of moisture content profiles computed for test problem 3 using mixed transform and modified Picard methods.

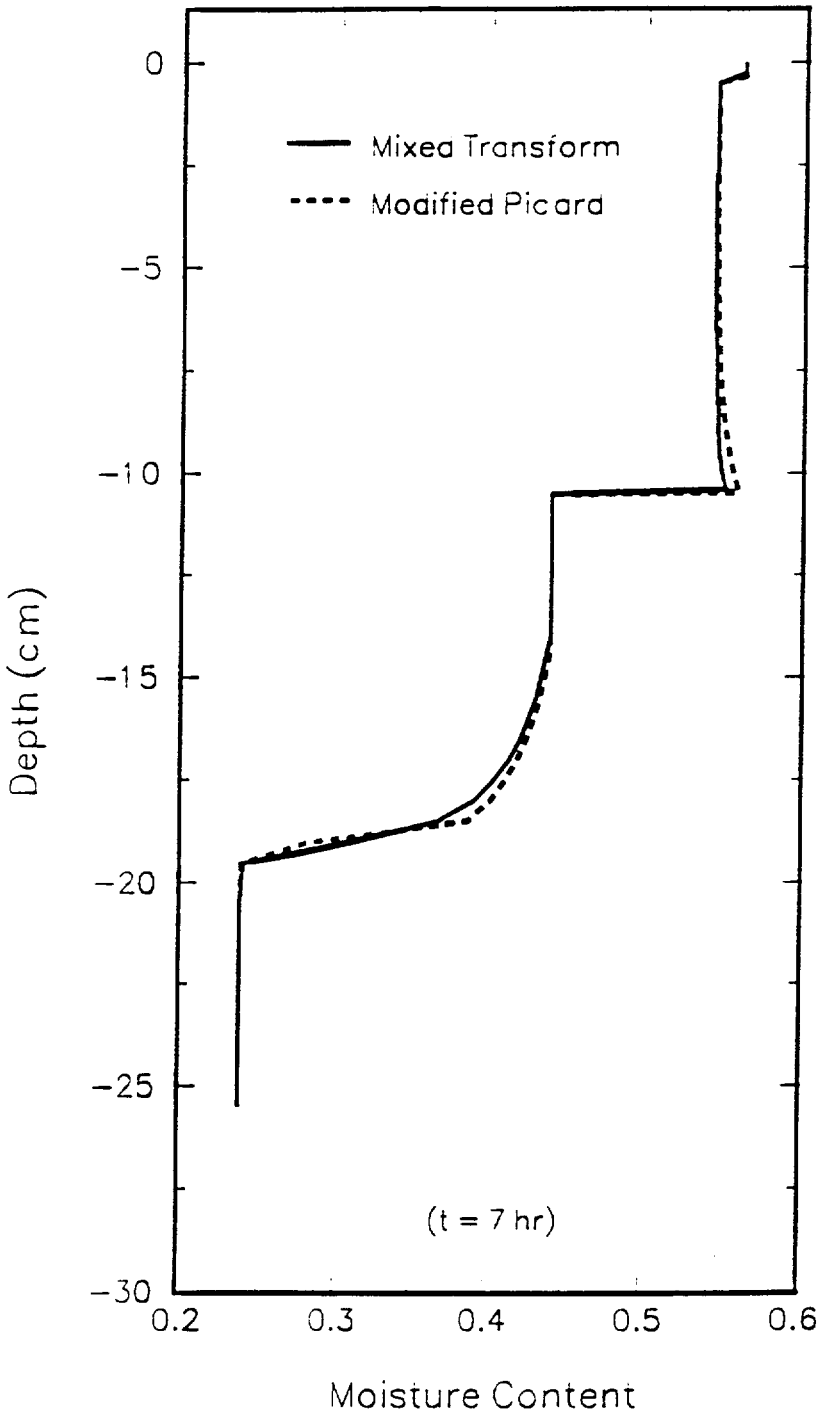

Fig. 8. Comparison of pressure head profiles computed for test problem 3 using mixed transform and modified Picard methods.

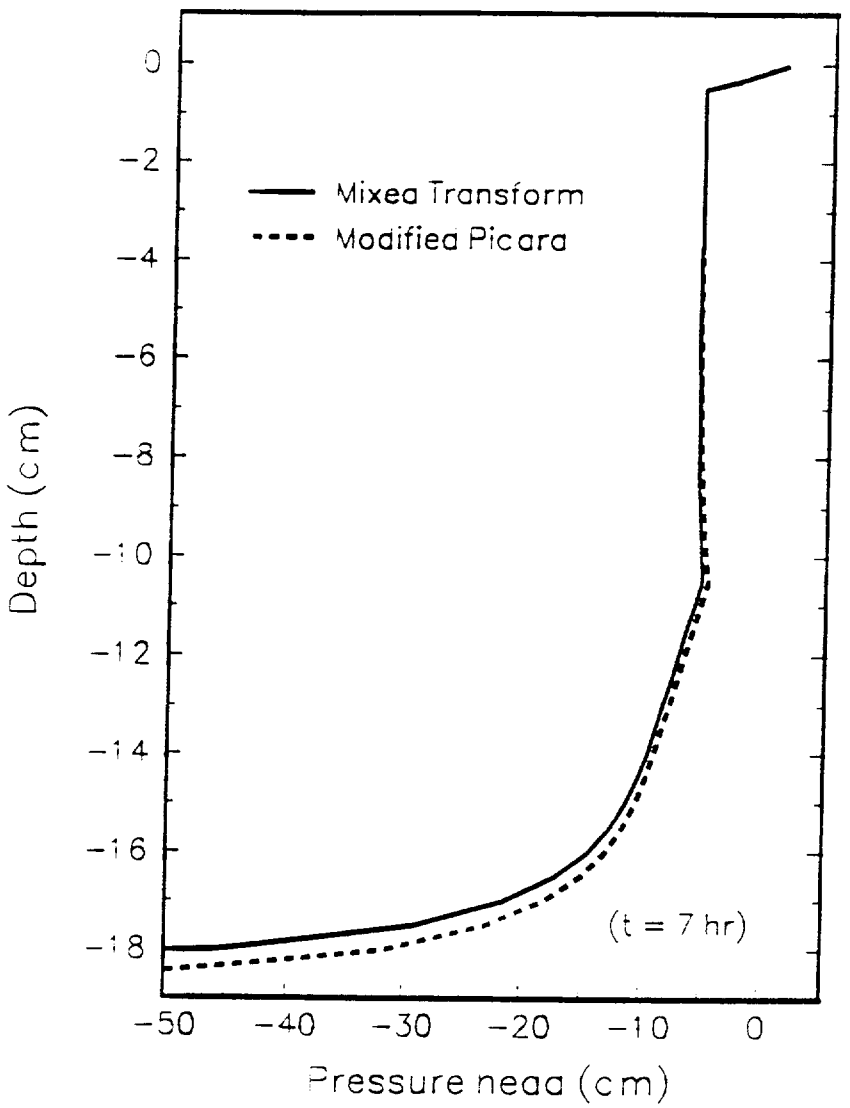

Fig. 9. Iteration histories computed for test problem 3 using the mixed transform and modified Picard method.